Finite difference analysis of transient flow through a staggered bundle of cylinders

L. Rorris, J. Rasoul, P. Anagnostopoulos, J. Ganoulis
Department of Civil Engineering, University of Thessaloniki, Thessaloniki 54006, Macedonia, Greece

ABSTRACT

The finite difference method was used for the solution of laminar incompressible flow through a staggered bundle of five cylinders in the streamwise direction. The two-dimensional Navier-Stokes equations were solved, in the formulation where the two components of the fluid velocity and the pressure are the field variables. The pitch to diameter ratio was 1.5, corresponding to equilateral triangular arrangement. The Reynolds numbers considered, based on the inflow velocity and the cylinder diameter, ranged between 50 and 200. Velocity profiles, streamline patterns, vorticity and pressure distributions and shear stress and pressure coefficients around the cylinders are presented.

INTRODUCTION

The investigation of flow through bundles of cylinders and spheres is a problem of growing engineering concern, since it is related to various engineering applications, such as heat exchangers, boilers, nuclear reactors, etc. It also provides an idealized tool for the investigation of flow through porous media at local scale, and gives insight to the microscopic flow properties such as the velocity and pressure distributions. Numerical investigations for flow through arrays of cylinders have been undertaken the last years, using finite difference or finite element techniques. Sangani and Acrivos [1] presented an analytical solution for the slow flow past periodic arrays of cylinders with application to heat transfer. Dhaubhadel et al. [2, 3] investigated the flow and heat transfer through bundles of cylinders of various arrangements, using a penalty finite element scheme. Ganoulis and Durst [4] simulated the flow through porous media using an array of closely spaced cylinders. For the sake of comparison they obtained a solution both with the finite element and the finite difference method. Ganoulis et al. [5] used Laser-Doppler anemometry for the measurement of velocity of flow through a periodic array of cylinders and compared the experimental measurements with numerical results at similar conditions.

Tezduyar and Liou [6] used the stream function and vorticity formulation for the finite element solution of flow through arrays of cylinders. Rasoul et al. [7] used the finite difference technique for the solution of laminar flow through an infinite depth staggered bundle of cylinders. They considered a unit cell in the streamwise direction and obtained by an iterative procedure the flow conditions when constant flow had been established after many wavelengths in the flow direction. The present paper deals with the numerical solution of transient flow through a staggered bundle of five cylinders.

In the present investigation the finite difference method was used for the solution of the Navier-Stokes equations for laminar flow of an incompressible fluid through a staggered bundle of cylinders, as shown in figure 1. An equilateral triangular arrangement was studied with pitch to diameter ratio P/D equal to 1.5 as shown in figure 1. The objective of the solution was the derivation of the flow pattern around the cylinders and the calculation of the pressure and shear stress distributions on the surface of these cylinders. The Reynolds numbers considered based on the inflow velocity and the cylinder diameter ranged between 50 and 200.

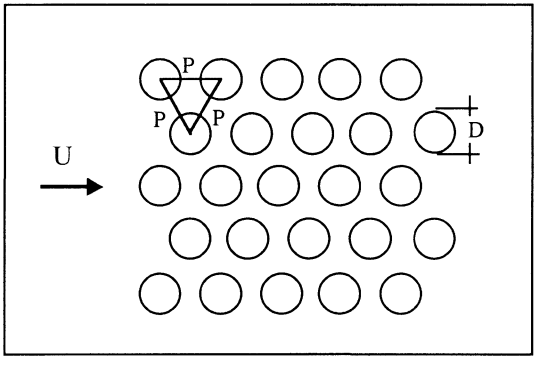

Figure 1. Geometry of an infinite staggered bundle of cylinders; P/D = 1.5.

NUMERICAL SOLUTION

The mathematical model of the problem consists of the Navier-Stokes and continuity equations. These equations can be written in the following non-dimensional form:

$$\frac{\partial u_i}{\partial t} + \frac{\partial (u_i u_j)}{\partial x_j} = -\frac{\partial p}{\partial x_i} + \frac{1}{Re}\nabla^2 u_i \qquad i=1,2; \quad j=1,2 \tag{1}$$

$$\frac{\partial u_j}{\partial x_j} = 0 \qquad j=1,2 \tag{2}$$

where

$$x_i = \frac{\bar{x}_i}{D}, \quad u_i = \frac{\bar{u}_i}{U}, \quad t = \frac{U\bar{t}}{D}, \quad p = \frac{\bar{p}}{\rho U^2}, \quad Re = \frac{UD}{\nu}$$

are the dimensionless variables; ν is the kinematic viscosity and ϱ is the fluid density; D is the cylinders diameter and U is the uniform velocity at the inflow boundary. In the following context the streamwise and cross-flow direction will be denoted by x and y and the two components of the fluid velocity by u and v.

The boundary conditions of the problem are explained with reference to figure 2:

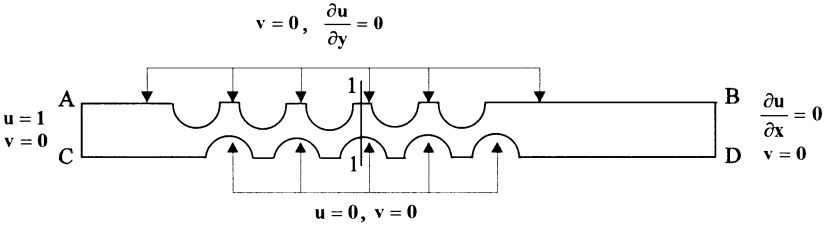

Figure 2. Solution domain and boundary conditions.

a) At the inlet boundary u = 1 and v = 0.
b) At the solid boundaries the non-slip condition dictates u = 0 and v = 0.
c) At the symmetry boundaries the u velocity profile is symmetric and the v component is zero; therefore $\partial u/\partial y = 0$, v = 0.
d) At the outlet boundary v = 0 and $\partial u/\partial x = 0$.

The finite difference technique applied herein is a variant of the artificial compressibility method proposed by Chorin [8] and Amsden and Harlow [9]. According to this method, perturbation velocities u_{ei} and pressure p_ϵ are introduced, satisfying the Navier-Stokes and the following non-dimensional form of the continuity equation:

$$\epsilon \frac{\partial p_\epsilon}{\partial t} + \frac{\partial u_{ej}}{\partial x_j} = 0 \qquad (3)$$

in which ε is a positive perturbation parameter close to zero. At every time step, an asymptotic numerical solution can be reached, so that the first term of equation 3 tends to zero. In this case the incompressibility condition (2) is satisfied and the perturbation velocities u_{ei} and p_ϵ tend to the real u_i and p. For the numerical integration of the perturbed system of equations the algorithm follows a fractional step computation, comprising the following steps:
1) An intermediate velocity field u_i^* is obtained from the momentum equation without the pressure gradient.
2) The pressure field is derived by iteration in a way that the equation (3) is satisfied.

3) The velocity field at the next time step is computed correcting the intermediate velocities u_i^* by the pressure gradient.
As initial condition for the solution at Reynolds numbers higher that 50 was taken the flow pattern for Re=6, because it was realized that it accelerated convergence. The computation continues, until steady state is reached.

A suitable staggered finite difference mesh was used for the numerical solution, with a step-like polygonal line for the approximation of solid boundaries. The distance between adjacent nodes in both directions was 1/30 of a cylinder diameter.

NUMERICAL RESULTS

As stated earlier the pitch to diameter ratio studied was equal to 1.5, at Reynolds numbers between 50 and 200. For each Reynolds number a laminar eddy appears behind each cylinder, growing continually with time until steady state is reached. From the velocity distribution the stream function Ψ and the vorticity ζ can be calculated throughout the flow field from the formulae

$$u = \frac{\partial \Psi}{\partial y}, \qquad v = -\frac{\partial \Psi}{\partial x}, \qquad \zeta = \frac{\partial v}{\partial x} - \frac{\partial u}{\partial y}$$

The computed profiles at section 1-1 of figure 2 of the two components of the fluid velocity at Re=50 normalized by the inflow velocity U are depicted in figure 3. From figure 3 we deduce that the u-velocity acquires a value as high as 4.25 U at y/D = 0.72, due to the restriction of the passage, while it becomes negative for y/D>1.1, due to the vortex formed behind the cylinder at the upper row. The v-velocity acquires its maximum value equal to 0.37 U at y/D=0.72, and becomes negative at y/D>1 in the region of the wake of the cylinder in the upper row.

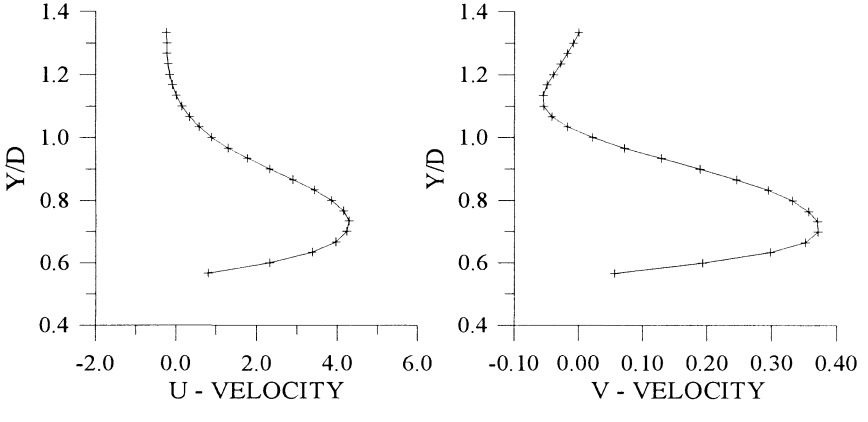

Figure 3. Velocity profiles at section 1-1 for Re=50.

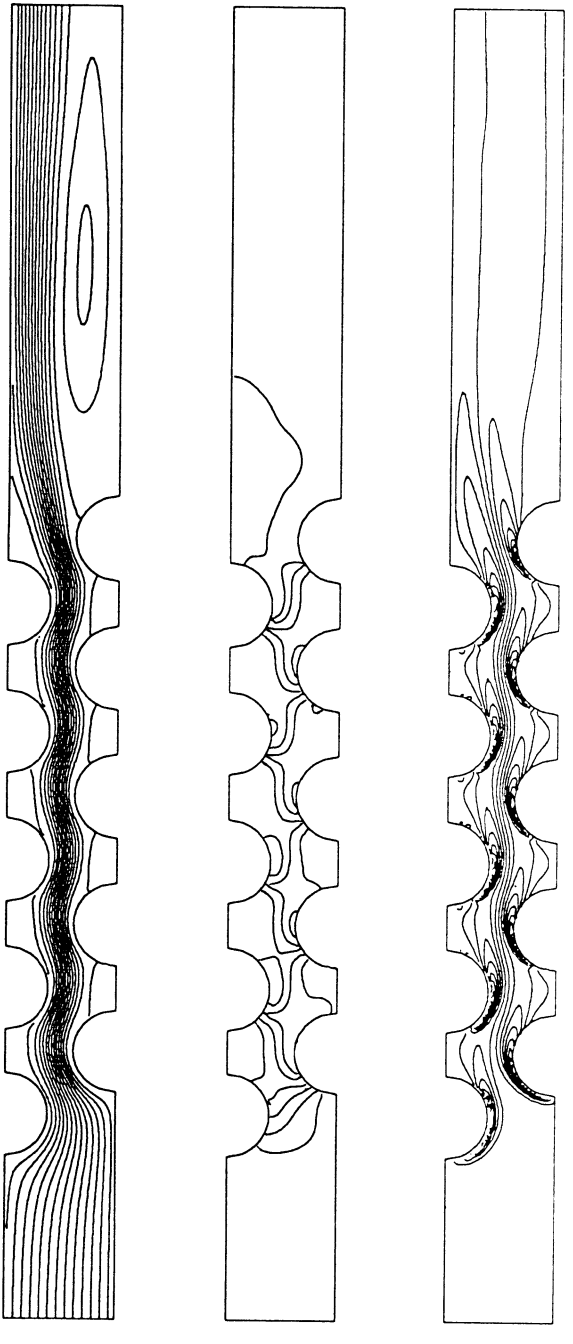

Figure 4. Streamlines, isobars and equivorticity lines for Re = 50.

The streamlines, isobars and equivorticity lines for Re=50 are presented in figure 4. The flow recirculates behind each cylinder, the size of the separation bubbles being suppressed from the next cylinder on the same row. Outside the separated region high velocities occur in the passage through the cylinders, as evident from the small spacing between adjacent streamlines. This result is in accord with continuity considerations, since the effective flow passage is greatly reduced. Behind the last cylinder of the lower row a large eddy is formed, extending almost to the outflow boundary. The vorticity has been calculated from the velocity field. The vorticity on the cylinders of the upper row is positive on the front part and negative in the separation zone, while negative vorticity prevails on the front part and positive in the separation zones of the cylinders of the lower row.

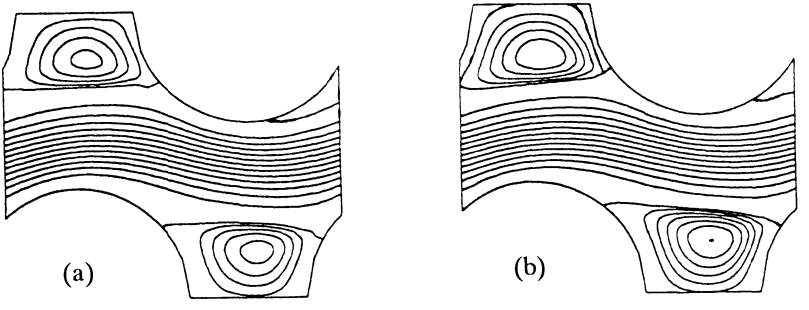

Figure 5. Enlarged view of streamlines. a) Re=50; b) Re=100.

An enlarged view of the streamlines in the region between the third and fourth cylinder is depicted in figure 5, for Re equal to 50 and 100. It is apparent from figure 5 that beyond the third cylinder the flow has become periodic and the separation eddy behind each cylinder increases with the Reynolds number.

The shear stress on the cylinder surface can be calculated from the formula

$$\tau = \mu \omega_B \tag{4}$$

where μ is the fluid viscosity and ω_B is the vorticity at the point considered. The non-dimensional shear stress coefficient c_f is calculated from the formula

$$c_f = \frac{2\tau}{0.5\,\rho\,U^2} \tag{5}$$

The shear stress coefficient distribution around each cylinder for Reynolds numbers 50 and 100 is presented in figure 6. A first observation is that the maximum value of c_f decreases with increasing Reynolds number. Moreover, the distribution of c_f is similar for the second, third and fourth cylinder. The shear stress coefficient is positive everywhere in the front part of the first cylinder, due to the absence of a separation eddy. Around the rear part of the fifth cylinder the values of c_f are lower than those of the previous cylinders, since the lack of

a cylinder downstream has as effect higher velocities and reduction of vorticity on that part of the cylinder.

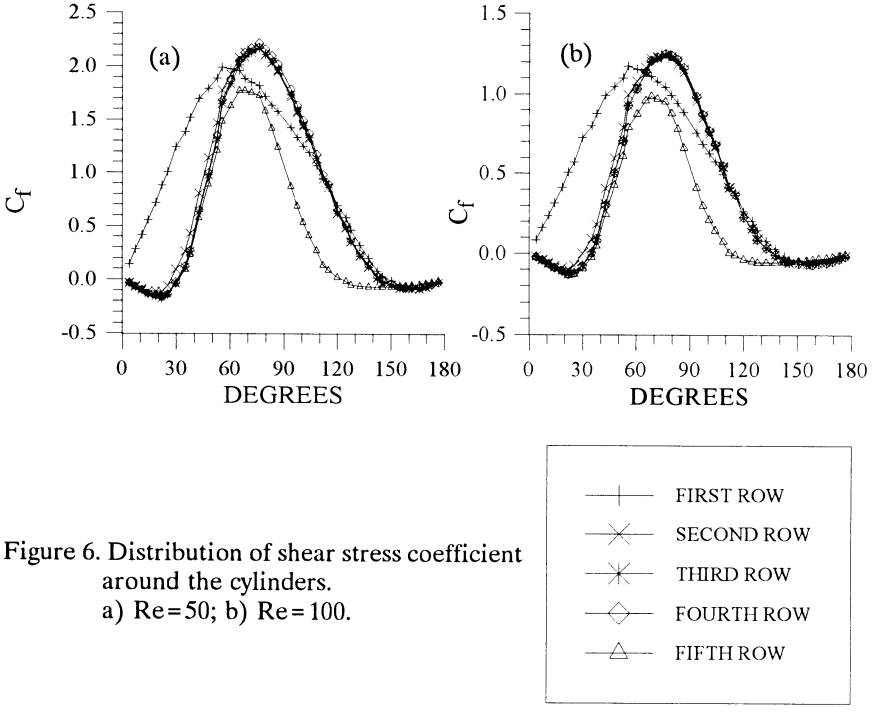

Figure 6. Distribution of shear stress coefficient around the cylinders.
a) Re=50; b) Re=100.

The non-dimensional pressure distributions around each cylinder at Reynolds numbers 50 and 100 are presented in figure 7. Since the pressure has

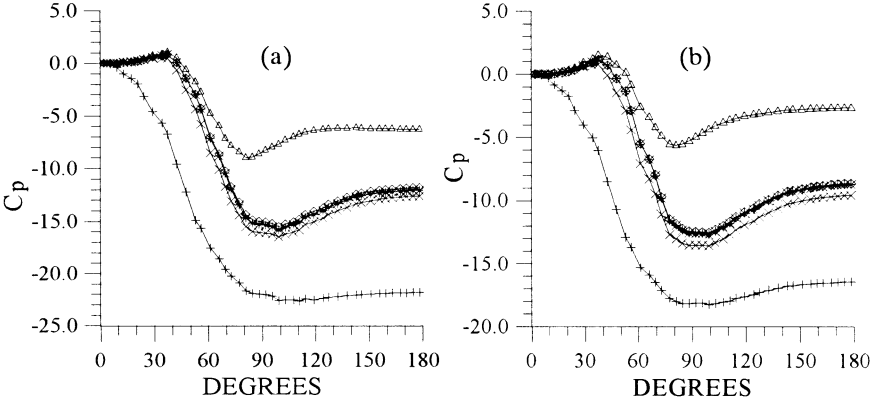

Figure 7. Distribution of pressure around the cylinders. a) Re=50; b) Re=100.

been normalized with respect to ϱU^2, the pressure coefficient is defined as $p\text{-}p_o$, where p_o is the pressure for $\phi = 0°$. Figure 7 indicates that the absolute c_p values are higher around the first cylinder, lower and almost similar around the next three cylinders while they become lowest around the fifth cylinder. The c_p values for Re = 50 are higher than the corresponding for Re = 100.

CONCLUSIONS

The finite difference scheme described herein was found to be a useful numerical tool for the solution of laminar flow through a staggered bundle of cylinders. The flow characteristics throughout the computational domain were presented and skin friction and pressure distribution around the cylinders were calculated. The separation eddies behind the cylinders increase in size as the Reynolds number increases, while the absolute values of the skin friction and pressure coefficient decrease with increasing Reynolds number. The flow after the fourth cylinder becomes periodic. The results of the present computation are in good agreement with those of a finite element solution at similar conditions [3].

REFERENCES

1. Sangani, A. S. and Acrivos, A. Slow flow past periodic arrays of cylinders with application to heat transfer, *International Journal of Multiphase Flow*, 1982, **8**, 193-206.
2. Dhaubhadel, M. N., Reddy, J. N. and Telionis, D. P. Penalty finite element analysis of coupled fluid flow and heat transfer for in-line bundle of cylinders in cross-flow, *International Journal of Non-Linear Mechanics*, 1986, **21**, 361-373.
3. Dhaubhadel, M. N., Reddy, J. N. and Telionis, D. P. Finite element analysis of fluid flow and heat transfer for staggered bundle of cylinders in cross-flow, *International Journal for Numerical Methods in Fluids*, 1987, **7**, 1325-1342.
4. Ganoulis, J. G. and Durst, F. Comparison between finite element and finite difference simulation of viscous flow through cylinders, in Proceedings of IV International Conference on Finite Elements in Water Resources, pp. 655-664, ed. Springer-Verlag Heidelberg, 1986.
5. Ganoulis, J., Brunn, P., Durst, F., Holweg, J., Wunderlich, A. Laser measurements and computations of viscous flow through cylinders, *Journal of Hydraulic Engineering*, ASCE, 1989, **115**, 1223-1239.
6. Tezduyar, T. E. and Liou, J. Computation of spatially periodic flows based on the vorticity-stream function formulation, *Computer Methods in Applied Mechanics and Engineering*, 1990, **83**, 121-142.
7. Rasoul, J., Anagnostopoulos, P. and Ganoulis, J. Numerical and experimental investigation of laminar flow through a staggered bundle of cylinders, *Zeitschrift Angewandte Mathematik und Mechanik*, 1994, to be published.
8. Chorin, A. J. A numerical method for solving incompressible viscous flow problems, *Journal of Computational Physics*, 1967, **2**, 12-21.
9. Amsden, A. A. and Harlow, F. H. Los Alamos Rep. No. La 4370, Los Alamos Nat. Lab., Los Alamos, N. M., 1970.